

Dual Band Wireless Power and Bi-Directional Data Link for Implanted Devices in 65 nm CMOS

Vamsi Talla¹, Vaishnavi Ranganathan¹, Brody Mahoney¹ and Joshua R. Smith^{1,2}

¹Dept. of Electrical Engineering and ²Dept. of Computer Science and Engineering, University of Washington, Seattle, USA.

Abstract—Implantable neural recording and stimulation devices hold great promise in monitoring and treatment of neurological disorders, limb reanimation and, development of brain-computer interfaces among other applications. However, transcutaneous wires limit the lifetime of such devices and there is a need for self-contained fully implantable solutions. In this work, we propose a novel dual-frequency approach for simultaneous wireless power transfer and low-power communication for small form factor fully implantable neural devices. We deliver wireless power using efficient magnetically coupled resonators operating at 13.56MHz and communicate using ultra-low power backscatter communication at 915 MHz. We leverage the frequency separation to combine wireless power and communication resonators with minimal interference using a novel concentric design, which meets the stringent size restrictions. We implement the wireless power receiver and communication front end of the implanted device in 65 nm CMOS and demonstrate 25 mW power delivery and 6 Mbps communication link.

I. INTRODUCTION

Neural recording and stimulation platforms hold great promise in developing solutions that may allow paralyzed individuals to operate motor prosthetic devices, effectively command electronic devices, or reanimate their limbs [1]. Recent advancements in microelectrode recording arrays, chip-based neural recording front ends and stimulation platforms have made significant strides towards these goals. However, the need for wires to connect the implanted system to an external unit through skull and skin for power and communication is a key deterrent against long-term use of such systems. The exit sites are highly prone to infection, limit the lifespan of the device and pose a risk to the health of the individual. The focus of this work is to eliminate wires by leveraging wireless power delivery and wireless communication.

Prior work on simultaneous wireless power and communication can be classified into two main categories: single antenna and multi antenna systems. Single antenna systems use one antenna/resonator operating at a single frequency for both near field wireless power transfer (WPT) and passive load modulation based communication. Load modulation for uplink is ultra-low power, however, it reduces the available power and creates a ripple at the output of a rectifier [2]. Additionally, downlink communication interferes with the power (ASK) and/or the recovered clock (PSK) at the receiver. Finally, there is a fundamental tradeoff between power transfer and communication. The efficiency of WPT is directly proportional to Q of the resonators and to achieve high WPT efficiency, high Q (i.e. low loss) resonators are used. On the other hand, communication data rate is inversely proportional to Q (low Q

results in higher bandwidth). As a result, efficient power transfer and high data rate communication cannot simultaneously co-exist on the same resonator. For example, authors in [2] demonstrate HF (1-13.56 MHz) power delivery of 100 mW but with very low data rate (10-100 KHz) communication. At UHF in [3], [4] high data rate communication (1 Mbps) is feasible but at the cost of low (10 μ W) power delivery.

An alternative approach is to use separate antennas for power transfer and communication. However, this requires careful design and placement of antennas since the system suffers from interference between power and communication. Prior work has addressed the interference issue by designing orthogonal or coplanar coils for 1-100 MHz HF band [5]–[8]. Although orthogonal and coplanar resonator topology reduces the crosstalk between the wireless power and communication subsystems, it increases the size of the implant, which is prohibitive in most cases. Additionally, these systems have focused on design of resonators [5]–[8] to minimize the interference due to cross-coupling but do not evaluate how the residual interference impacts the communication performance. [6] proposed a coplanar coil topology with high speed OQPSK downlink but the system requires a power hungry receiver on the implant which is impractical for implanted systems. Finally, the systems are designed for wireless power and downlink and do not address high data rate, ultra-low power uplink communication which is required for applications such as neural recording systems. [5] proposed an active UWB radio for uplink communication, but is undesirable since it increases the power consumption of the implant. In this work, we propose a simultaneous wireless power and bi-directional wireless communication solution for miniature-implanted systems. We use a multi-antenna topology but instead of using orthogonal or coplanar coils we use orthogonal frequency bands for wireless power data transfer and backscatter communication to minimize interference. We note that WPT at HF frequencies is highly efficient (lower attenuation) and communication at higher frequencies has larger bandwidth, which can support high data rates. We combine the benefits of WPT at HF and backscatter communication at UHF for simultaneous WPT and communication at high data rates. We propose a novel concentric WPT and UHF receiver antenna configuration to conform to the stringent form factor requirements of implanted systems. Finally, we introduce low power techniques to mitigate residual interference on the communication link. We implement the wireless power receiver and communication front end on the implanted device in 65 nm CMOS, and demonstrate 25 mW

power delivery and 6 Mbps communication link.

II. SYSTEM DESIGN

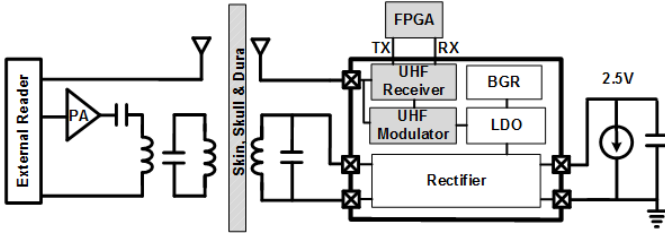


Fig. 1. Top level architecture of proposed approach for simultaneous WPT and bi-directional communication

Our system targets a fully implantable ElectroCorticography (ECoG) platform. ECoG is a procedure for recording the electrical activity of the brain using electrodes placed on the surface of the cerebral cortex. It has been shown that ECoG electrodes are more suitable for long-term recordings than intra-cortical electrodes, as ECoG recording is less affected by electrode movement and tissue response [1]. Typical ECoG platforms which support up to 64 recording channels (each sampled at 1KHz with 16-bit precision/sample), consume 225 μW and require 1 Mbps communication link [9]. However, as the number of recording channels scale and stimulation channels are added to the same platform, the requirements for power and data rates will scale proportionately. In this work, we propose a scalable solution, which can simultaneously deliver high power wirelessly and achieve ultra-low power high data rate wireless communication. We deliver up to 25 mW of power and achieve 6 Mbps uplink communication at a separation of 1 cm. However, we believe this scalable technique can be used in future work to deliver higher power and achieve higher data rates.

We first describe the design and implementation of WPT followed by UHF backscatter communication and interference mitigation strategies. The top level architecture of the system is shown in Fig. 1.

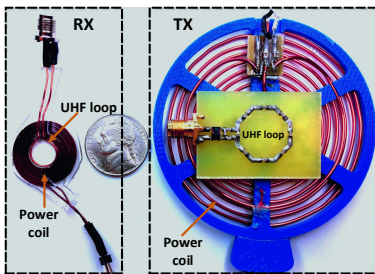


Fig. 2. Transmit and receive resonators for simultaneous WPT and bi-directional communication

A. Near Field Wireless Power Transfer

A three coil magnetically coupled resonator topology operating at 13.56 MHz is used for WPT between an external transmitter and the implanted miniature coils. The key advantage

of resonant coupling is that adaptation techniques such as frequency tuning (used in this work) and impedance matching can be used to efficiently deliver power. The volume constraints of brain cavity (2 cm diameter and 2 mm thick cavity for implants in non-human primates) impose stringent size constraints on the implanted system. We use a 2 cm diameter flat pancake coil made using 24 AWG copper wire encapsulated in PDMS as the receive resonator coil ($Q \approx 90$ in air) [10]. On the transmitter, we use 18 AWG 6.5 cm diameter loop and a coil ($Q \approx 300$ in air). Transmit and receive resonators are optimized for an operating range of 7-10 mm. The receive resonator is tuned by an external capacitor and connected to an on-chip HF rectifier. The technique to compensate for tissue-induced detuning of resonators presented in [11] can be used to achieve high WPT efficiencies with implanted coils. We implement a PMOS cross coupled switch and active deep-n-well NMOS rectifier using thick oxide I/O devices in 65 nm CMOS process [12]. The rectifier was optimized for mW power delivery and achieves an efficiency of 80% for 25 mW output power. The rectified output is regulated by a 1 V LDO which powers the communication and recording subsystems. We skip the circuit details for brevity.

B. UHF Bi-directional Backscatter Communication

Backscatter communication at 915MHz is a perfect fit for neural implants that require low data rate downlink for sending commands and high data rate uplink to stream the recorded signals. For downlink, we use amplitude modulation with pulse interval encoding at 160 kbps similar to an RFID reader. Since the implant is power constrained, active radios on the receiver are undesirable. Our receiver uses a charge pump based envelope detector followed by RC filters and a low power comparator to decode the bits. Uplink uses backscatter communication, wherein the implant switches the impedance at the receive UHF antenna between matched and short states to transmit bits. The external reader transmits the carrier wave and detects the change in reflected signal to decode the backscatter bits which are encoded using FM0 at 6 Mbps. The reader implements time-domain multiplexing to avoid collision between down and uplink. The distance between transmitter and receiver is limited to 1 cm in ECoG applications, which is in the near field at 915 MHz. We use an 8 mm diameter loop antenna at the receiver and a segmented loop antenna for the transmitter [13] as shown in Fig. 2.

C. System Integration and Suppressing Interference

On the transmit side, we prioritize HF power and place the UHF segmented loop antenna behind the HF power coil. This configuration significantly improves the efficiency of WPT (compared to when the HF power coil is placed behind) and has minimal impact on the link budget of communication, which can be compensated with a nominal increase in the reader's transmit power.

On the receive side, we place the UHF coil concentrically inside the HF resonator, as shown in Fig. 2, to conform to the size restrictions. Concentrically placed coils have high

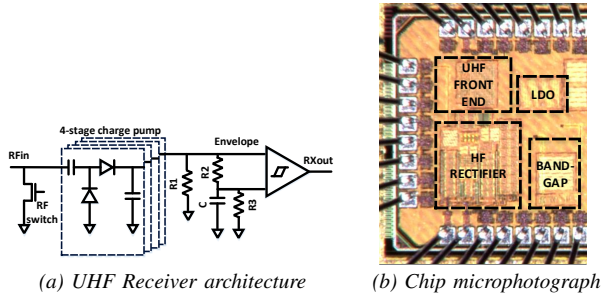


Fig. 3. The architecture of the UHF receiver and the microphotograph of the 65nm CMOS die.

coupling coefficient, which can lead to significant interference between wireless power and communication. We leverage separation in the frequency domain to minimize interference. First, since we are exclusively using UHF band for near field communication, the UHF reader transmit power is low and as a result, communication has negligible impact on WPT. Additionally, magnetically coupled resonators are extremely frequency selective (high-Q band-pass for efficient power transfer) and rectifiers have μF filtering capacitors at the output which makes WPT immune to interference at UHF.

On the other hand, the output power at HF is in the order of 100 mW which causes significant interference on the UHF communication link operating at μW signal levels. To suppress this strong interference on downlink communication, first we use a high Q LC filter to match the receiver front end to the impedance of the UHF antenna ($6.7 - j63.9$), which provides first level of filtering. Secondly, at the output of the four stage charge pump based envelope detector, we add additional band pass filtering which passes 160 kbps downlink data but suppresses the HF interference as shown in Fig. 3(a). Finally, we make a design choice to trade the sensitivity of the receiver by introducing an offset in the comparator to counter any residual interference at the input of the comparator. For uplink communication, the band pass characteristics of LNA, mixers and baseband filters of the active radio chain on the external UHF backscatter reader suppresses the minimal interference from WPT in the UHF band. The receiver and transmitter on the implant side consumes an average of $2 \mu W$ and $950 nW$ respectively during typical operation. The baseband protocol is implemented on an FPGA and interfaced with the chip.

III. RESULTS

The HF rectifier and the UHF transceiver on the implant is implemented in TSMC 65nm GP CMOS process. An annotated die microphotograph is shown in Fig. 3(b). The baseband protocol was implemented on a DE1 Altera FPGA and interfaced with the UHF front end. On the transmit side, a commercial power amplifier (100W1000B by AR) was used as the power source and the UHF backscatter reader was implemented on a USRP N210 software defined radio. The proposed system is optimized to minimize the interference between wireless power and communication. In the interest of space, we evaluate the system in the worst-case scenario for WPT, which would result in maximum interference. The

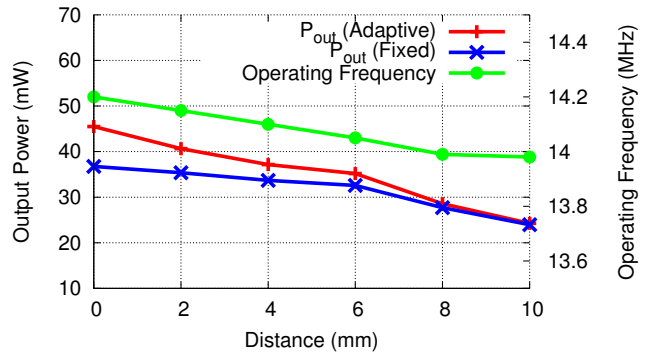


Fig. 4. **HF Wireless Power Transfer.** Maximum available power at the output of the rectifier at 1.2 V. The plot shows the performance with adaptive frequency tuning and fixed operating frequency.

output of the rectifier feeds a 1 V LDO which requires a minimum input voltage of 1.2 V. At 1.2 V output, the rectifier is highly inefficient (less than 50% due to 600 mV diode threshold) and the LDO is at the edge of it's operation which equates to the worst case WPT efficiency. We simulate this configuration in our experiments by connecting the output of the rectifier to a source measuring unit and set it to 1.2 V (200 mV LDO dropout) and measure the load current. We set the PA to deliver an output power of 200 mW to a 50Ω load which supports a minimum load of 25 mW at the maximum operating range of 1 cm. The following experiments are run with the HF PA and UHF reader operating simultaneously.

A. HF Wireless Power Transfer

We vary the distance between transmit and receive resonators and implement frequency tracking to track maximum power delivery. Fig. 4 shows that as the distance increases, the available power decreases due to reduction in coupling between the transmitter and receiver. Up to a distance of 8 mm (critical coupling point), frequency tracking algorithm delivers higher power to the receiver compared to fixed frequency operation. Beyond 8 mm, frequency tracking algorithm converges to the fixed operating frequency of 13.93 MHz.

B. UHF Backscatter Communication

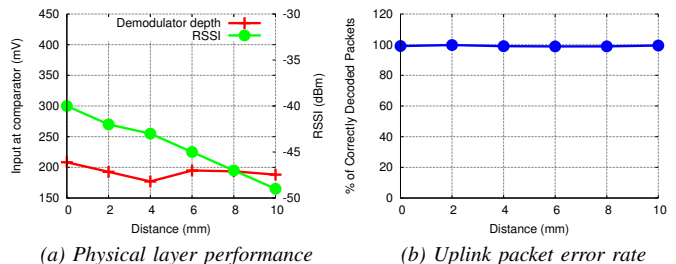


Fig. 5. Near field UHF bi-directional communication performance.

Next, we show the efficacy of UHF bi-directional communication between the chip and the external backscatter reader at 160 kbps downlink and 6 Mbps uplink data rates. We set the output power of the reader to -5 dBm (for operation up to 1 cm) and vary the distance between transmit and receive

TABLE I
COMPARISON WITH STATE OF THE ART

References	Configuration	Power	Communication	Delivered Power	Uplink	Downlink	Process
This Work	Concentric coils	13.56 MHz Near Field with freq. tuning	Bi-directional 915 MHz Backscatter	25 mW @ 1 cm	6 Mbps @ 950 nW	160 kbps @ 2 μ W	65 nm GP CMOS
[6]	Coplanar coils	1 MHz Near Field	Downlink 13.56 MHz Near Field	10-100 mW (RF output)	NA	4.16 Mbps [†]	NA
[3]	Single coil	1.5 GHz Near Field	Bi-directional 1.5 GHz Backscatter	10.5 μ W @ 1 mm	1 Mbps @ 200 nW *	200 kbps @ 2 μ W *	65 nm LP CMOS
[9]	Single coil	300 MHz Near Field	Uplink 1.5 GHz Backscatter	225 μ W @ 1 cm	1 Mbps @ 2.4 μ W (with encoder)	NA	65 nm LP CMOS

* Estimated [†] Power data not available

resonators. Fig. 5(a) shows the received signal at the envelope detector and the RSSI of the backscatter uplink data receiver by the backscatter reader. It can be seen that the signal strength decreases as the separation between transmit and receive antennas is increased. Moreover, the link budget for uplink communication is far greater than the sensitivity of typical readers (-85 dBm) which means either the transmit power can be reduced and/or higher data rate uplink communication can be supported with this configuration. Finally, Fig. 5(b) shows that percentage of packets correctly decoded on the reader to demonstrate the successful performance of the uplink communication up to a distance of 1 cm.

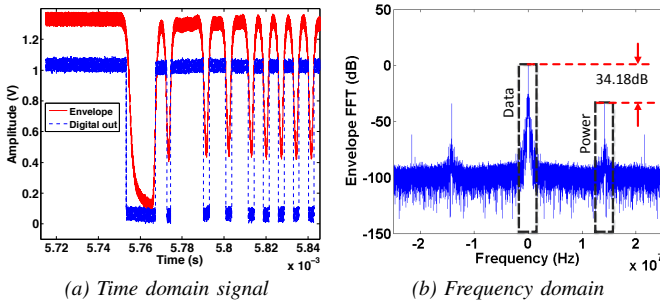


Fig. 6. Co-existence of WPT and communication

C. Co-existence of WPT and Communication

Finally, we measure interference between WPT and communication. As expected, we notice that there is no interference due to communication on the output of the rectifier and similarly, there is no impact of WPT on the uplink communication. We study the impact of WPT on downlink communication by measuring the input to the receive comparator. This signal is shown in both time and frequency domain in Fig. 6. We notice a small 13.93 MHz signal riding on top of the time domain signal at the output of the envelope detector and band pass filter. However, the additional offset in the comparator filters this interference to correctly decode the downlink data. The frequency domain plot shows that the interference from the power (25 mW received) is 34 dB lower than the average power of the downlink data.

IV. CONCLUSION

We have introduced a new approach and novel concentric antenna configuration for simultaneous wireless power transfer and wireless communication for implanted systems. Table I shows a comparison of our work with similar form factor state

of the art solutions. By leveraging the benefits of wireless power transfer at HF and high data rate ultra low power backscatter communication at UHF, we have created a solution which can enable large-scale fully implanted systems.

V. ACKNOWLEDGMENT

This work was funded by NSF (EEC-1028725), Allen Family Foundation and Intel Fellowship.

REFERENCES

- [1] E. C. Leuthardt, G. Schalk, J. R. Wolpaw, J. G. Ojemann, and D. W. Moran, "A brain-computer interface using electrocorticographic signals in humans," *Journal of neural engineering*, vol. 1, no. 2, p. 63, 2004.
- [2] M. Ghovanloo and S. Atluri, "An integrated full-wave cmos rectifier with built-in back telemetry for rfid and implantable biomedical applications," *Circuits and Systems I: Regular Papers, IEEE Transactions on*, vol. 55, no. 10, pp. 3328–3334, 2008.
- [3] W. Biederman, D. Yeager, N. Narevsky, A. Koralek, J. Carmena, E. Alon, and J. Rabaey, "A fully-integrated, miniaturized (0.125 mm²;) 10.5 μ W wireless neural sensor," *Solid-State Circuits, IEEE Journal of*, vol. 48, no. 4, pp. 960–970, April 2013.
- [4] S. J. Thomas, R. R. Harrison, A. Leonardo, and M. S. Reynolds, "A battery-free multichannel digital neural/emg telemetry system for flying insects," *Biomedical Circuits and Systems, IEEE Transactions on*, vol. 6, no. 5, pp. 424–436, 2012.
- [5] U.-M. Jow and M. Ghovanloo, "Optimization of data coils in a multi-band wireless link for neuroprosthetic implantable devices," *Biomedical Circuits and Systems, IEEE Transactions on*, vol. 4, no. 5, pp. 301–310, 2010.
- [6] G. Simard, M. Sawan, and D. Massicotte, "High-speed oqpsk and efficient power transfer through inductive link for biomedical implants," *Biomedical Circuits and Systems, IEEE Transactions on*, vol. 4, no. 3, pp. 192–200, 2010.
- [7] A. K. RamRakhyani and G. Lazzi, "On the design of efficient multi-coil telemetry system for biomedical implants," *Biomedical Circuits and Systems, IEEE Transactions on*, vol. 7, no. 1, pp. 11–23, 2013.
- [8] G. Wang, P. Wang, Y. Tang, and W. Liu, "Analysis of dual band power and data telemetry for biomedical implants," *Biomedical Circuits and Systems, IEEE Transactions on*, vol. 6, no. 3, pp. 208–215, 2012.
- [9] R. Muller, H.-P. Le, W. Li, P. Ledochowitsch, S. Gambini, T. Bjorninen, A. Koralek, J. M. Carmena, M. M. Maharbiz, E. Alon *et al.*, "A minimally invasive 64-channel wireless μ cog implant," *Solid-State Circuits, IEEE Journal of*, vol. 50, no. 1, pp. 344–359, 2015.
- [10] V. Talla and J. R. Smith, "An experimental technique for design of practical wireless power transfer systems," in *Circuits and Systems (ISCAS), 2014 IEEE International Symposium on*. IEEE, 2014, pp. 2041–2044.
- [11] V. Talla, B. Waters, and J. Smith, "A study of detuning effects and losses in implantable coils for biomedical wireless power transfer," *Session 4A4 SC4: Wireless Energy Transmission and Harvesting*, p. 1369, 2013.
- [12] Y.-H. Lam, W.-H. Ki, and C.-Y. Tsui, "Integrated low-loss cmos active rectifier for wirelessly powered devices," *Circuits and Systems II: Express Briefs, IEEE Transactions on*, vol. 53, no. 12, pp. 1378–1382, 2006.
- [13] J. S. Besnoff and M. S. Reynolds, "Near field modulated backscatter for in vivo biotelemetry," in *RFID (RFID), 2012 IEEE International Conference on*. IEEE, 2012, pp. 135–140.